

Mixed Convection in a Tilted Lid-Driven Square Enclosure with Adiabatic Cylinder at the Center

Sumon Saha^a, Ahmed Kadhim Hussein^{*,b}, Goutam Saha^c and Salam Hadi Hussain^d

^aDepartment of Mechanical Engineering, The University of Melbourne, Parkville, VIC 3010, Australia

^{b,d} Department of Mechanical Engineering, College of Engineering, Babylon University, Babylon Province, Iraq

^cDepartment of Mathematics, The University of Dhaka, Dhaka 1000, Bangladesh

*Corresponding author: ahmedkadhim74@yahoo.com (A. K. Hussein)

ABSTRACT

The problem of two-dimensional laminar mixed convection in a tilted lid-driven square enclosure in the presence of adiabatic cylinder at the center is formulated and studied numerically using the combined finite element method. In the present investigation, parametric studies are carried out for the variation of the inclination angles and Richardson numbers, while keeping Reynolds number equal to 100 and Prandtl number equal to 0.71 for the air. Fluid flow and heat transfer characteristics via streamlines, isotherms and average Nusselt number are also presented. The results indicate that for all Richardson numbers considered in the present study, the flow and thermal fields eventually reach the steady state with the symmetric shape about the vertical centerline through the center of the inner circular cylinder. It is also observed that the inclination angle of the enclosure is an important parameter affecting the fluid flow and heat transfer characteristics.

Keywords: Free and mixed convection; lid-driven enclosure; adiabatic cylinder; Nusselt number; buoyancy driven flow; Richardson number.

1. INTRODUCTION

Analysis of mixed convective flow in a lid-driven cavity finds applications in cooling of electronic devices, lubrication technologies, drying technologies, food processing, float glass production, flow and heat transfer in solar ponds, thermal hydraulics of nuclear reactors, dynamics of lakes, crystal growing, metal coating, reservoirs and cooling ponds, materials processing etc. There have been many investigations in the past on mixed convective flow in lid-driven cavities. Mohammad and Viskanta [1] predicted the flow and heat transfer in a shallow, lid-driven cavity with a low Prandtl number fluid. They considered the cavity

either heated from below and cooled from above or one heated from above and cooled from below. Moallemi and Jang [2] numerically studied mixed convection flow in a bottom heated square driven cavity and investigated the effect of Prandtl number on the flow and heat transfer process. Iwatsu *et al.* [3] and Iwatsu and Hyun [4] conducted two and three-dimensional numerical simulation of mixed convection in square cavities heated from the top moving wall. Mansour and Viskanta [5] studied mixed convective flow in a tall vertical cavity where one of the vertical side walls, maintained at a lower temperature than the other, was moving up or downward thus assisting or opposing the buoyancy. Prasad and

Koseff [6] reported experimental results for mixed convection in deep lid-driven cavities heated from below. Kuhlmann *et al.* [7] conducted a numerical and experimental study on steady flow in rectangular two sided lid-driven cavities. They found that the basic two-dimensional flow was not always unique. Alleborn *et al.* [8] numerically investigated mixed convection in a shallow cavity with a moving heated lid at the bottom and a moving cold lid at the top in a process engineering context of drying. They determined the effect of Reynolds number and concentration in cavities at different angles. Khanafer and Chamkha [9] examined numerically mixed convection flow in a lid-driven enclosure filled with a fluid saturated porous medium and reported on the effects of the Darcy and Richardson numbers on the flow and heat transfer characteristics. Shankar *et al.* [10] presented analytical solution for mixed convection in cavities with very slow lid motion. The convection process was shown to be governed by an inhomogeneous biharmonic equation for the stream-function. Oztop and Dagtekin [11] performed numerical analysis of mixed convection in a square cavity with moving and differentially heated sidewalls.

Buoyancy driven flow and heat transfer between a cylinder and its surrounding medium has been a problem of considerable importance. This problem has a wide range of applications. Energy storage devices, crop dryers, crude oil storage tanks, heat exchangers and spent fuel storage of nuclear power plants are a few examples to mention. Larson *et al.* [12] carried out experimental study of temperature field around a heated horizontal cylindrical body in an isothermal rectangular

enclosure. Roychowdhury *et al.* [13] analyzed the natural convective flow and heat transfer features for a heated cylinder kept in a square enclosure with different thermal boundary conditions. Elepano and Oosthuizen [14] carried out numerical study of natural convective flow in an enclosure containing a heated cylinder and a cooled upper surface. Kim *et al.* [15] performed a numerical study of natural convection in a cooled square enclosure with an inner heated circular cylinder. The results indicated that the number, shape and formation of the cell were dependant on the inner circular cylinder position and the Rayleigh number. Misirlioglu [16] studied the heat transfer in a square cavity filled with clear fluid or porous medium where a rotating circular cylinder was placed at the centre of the cavity. The results showed that rotation was more effective in the forced convection regime than in mixed and natural convection regimes. Recently, Hussain and Hussein [17] performed a numerical study of two-dimensional steady natural convection where a uniform heat source applied on the inner circular cylinder in a square air filled enclosure in which all boundaries were assumed to be isothermal. The numerical solutions revealed a two cellular flow field between the inner cylinder and the enclosure.

A majority of the available studies [18–20] deal with natural convective flow and heat transfer around a circular cylinder kept inside an enclosure. There has been little study on the mixed convection process with insulated cylinder inside an inclined enclosure with cold side walls. So far, Saha *et al.* [21] performed numerical investigation with insulated cylinder inside enclosure but they considered natural convection problem with discrete

heating and the effect of inclination angle on flow and thermal field was not analyzed. In the present analysis mixed convection of flow and heat transfer in a tilted lid-driven square enclosure with adiabatic cylinder at the center; cooled from the moving sidewalls, bottom wall is maintained at a constant heat flux and top wall remains adiabatic has been studied to examine the effect of heat transfer process in a tilted lid-driven enclosure with adiabatic cylinder at the center. The results are shown in terms of parametric presentations of streamlines and isotherms plot in the enclosure. Also the effects of various dimensionless parameters and inclination angles on the heat transfer process are analyzed and the results are presented in terms of the average Nusselt number.

2. PROBLEM FORMULATION

Here the steady, laminar, incompressible and combined forced-free convection flow in a two-dimensional tilted lid-driven square enclosure of length H has been considered. The physical model and coordinate system considered in this investigation are shown in Figure 1. Both the sidewalls are moving downward with a uniform velocity, V_0 and are kept at a constant temperature, T_c , the top wall is adiabatic and the bottom wall is maintained at a constant heat flux, q . The cylinder having a radius of $(H/5)$, is placed at the center of the square enclosure and no slip boundary condition is assumed on the cylinder surface.

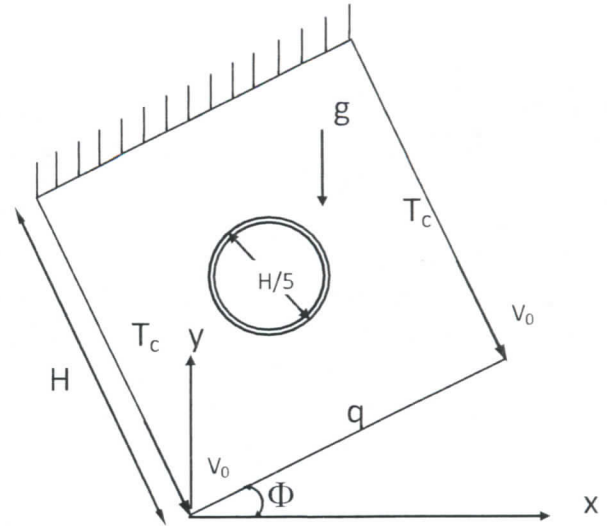


Figure 1: Schematic diagram of the physical domain

2.1 Governing Equations

Mixed convection is governed by the differential equations expressing conservation of mass, momentum and energy. The present flow is considered steady, laminar, incompressible and two-dimensional. The viscous dissipation term in the energy equation is neglected. The Boussinesq approximation is invoked for the fluid properties to relate density changes to temperature changes, and to couple the temperature field with the flow field. Then the governing equations for steady mixed convection can be expressed in the dimensionless form as:

$$\frac{\partial U}{\partial X} + \frac{\partial V}{\partial Y} = 0 \quad (1)$$

$$U \frac{\partial U}{\partial X} + V \frac{\partial U}{\partial Y} = -\frac{\partial P}{\partial X} + \frac{1}{\text{Re}} \left(\frac{\partial^2 U}{\partial X^2} + \frac{\partial^2 U}{\partial Y^2} \right) + (Ri \sin \Phi) \theta \quad (2)$$

$$U \frac{\partial V}{\partial X} + V \frac{\partial V}{\partial Y} = -\frac{\partial P}{\partial Y} + \frac{1}{\text{Re}} \left(\frac{\partial^2 V}{\partial X^2} + \frac{\partial^2 V}{\partial Y^2} \right) - (Ri \cos \Phi) \theta \quad (3)$$

$$U \frac{\partial \theta}{\partial X} + V \frac{\partial \theta}{\partial Y} = \frac{1}{\text{RePr}} \left(\frac{\partial^2 \theta}{\partial X^2} + \frac{\partial^2 \theta}{\partial Y^2} \right) \quad (4)$$

where, X and Y are the coordinates varying along horizontal and vertical directions respectively, U and V are the non-dimensional velocity components in the X and Y directions, θ is the non-dimensional temperature and P is the non-dimensional pressure. The non-dimensional numbers Ri , Re and Pr are the Richardson number, Reynolds number and Prandtl number respectively and they are mathematically represented as,

$$Ri = \frac{g\beta\Delta TH}{V_o^2}, Re = \frac{V_o H}{\nu}, Pr = \frac{\nu}{\alpha} \quad (5a)$$

The dimensionless parameters in the equations above are defined as follows:

$$X = \frac{x}{H}, Y = \frac{y}{H}, U = \frac{u}{V_o}, V = \frac{v}{V_o}, P = \frac{p}{\rho V_o^2}, \quad (4)$$

$$\theta = \frac{T - T_c}{\Delta T}, \Delta T = \frac{qH}{k} \quad (5b)$$

where ρ , β , ν , α , and g are the fluid density, coefficient of volumetric expansion, kinematic viscosity, thermal diffusivity and gravitational acceleration respectively.

2.2 Boundary conditions

The boundary conditions for the present problem are specified as follows:

1. For top wall: $\partial\theta/\partial Y = 0$, $U = V = 0$.
2. For bottom wall: $\partial\theta/\partial Y = -1$, $U = V = 0$.
3. In case of vertical sidewalls: $\theta = 0$, $U = 0$ and $V = -1$
4. For cylinder surface: $U = V = 0$ and $\partial\theta/\partial S = 0$.

The average Nusselt number at the heated wall of the enclosure may be expressed by the following equation:-

$$Nu = \int_0^1 \frac{1}{\theta_s(x)} dX \quad (6)$$

where $\theta_s(X)$ is the local dimensionless hot surface temperature.

3. Finite Element Formulation

The six-node triangular element is used in this study. The element assumes linear interpolation for the velocity components, the pressure and the temperature as follows:

$$U(X, Y) = N_i U_i \quad (7a)$$

$$V(X, Y) = N_i V_i \quad (7b)$$

$$P(X, Y) = N_i P_i \quad (7c)$$

$$\theta(X, Y) = N_i \theta_i \quad (7d)$$

where, $i = 1, 2, 3, 4, 5, 6$ and N_i is the element interpolation functions. The basic idea of the solution algorithm proposed in this paper is to use the two momentum equations for solving both of the velocity components, the continuity equation for solving the pressure and the energy equation for solving the temperature.

3.1 Discretization of the momentum equations

The two momentum equations (2) and (3) are discretized using the conventional Bubnov-Galerkin's method. However, a special treatment of the convection terms is incorporated. Using the standard Galerkin approach, each momentum equation is multiplied by weighting functions, N_i and then the diffusion terms are integrated by parts using the

Gauss theorem to yield the finite element equations in the form,

$$AU = R_{pX} + R_U + R_a \quad (8a)$$

$$AV = R_{pY} + R_V + R_b \quad (8b)$$

where, the coefficient matrix A contains the known contributions from the convection and diffusion terms. The load vectors on the right-hand side of Eqs. (8a) and (8b) are defined by,

$$R_{pX} = - \int_{\Omega} N_i \frac{\partial P}{\partial X} d\Omega \quad (9a)$$

$$R_{pY} = - \int_{\Omega} N_i \frac{\partial P}{\partial Y} d\Omega \quad (9b)$$

$$R_U = \frac{1}{\text{Re}} \int_{\Gamma} N_i \left(\frac{\partial U}{\partial X} n_x + \frac{\partial U}{\partial Y} n_y \right) d\Gamma \quad (9c)$$

$$R_V = \frac{1}{\text{Re}} \int_{\Gamma} N_i \left(\frac{\partial V}{\partial X} n_x + \frac{\partial V}{\partial Y} n_y \right) d\Gamma \quad (9d)$$

$$R_a = \int_{\Omega} N_i (Ri \sin \Phi \theta) d\Omega \quad (9e)$$

$$R_b = \int_{\Omega} N_i (Ri \cos \Phi \theta) d\Omega \quad (9f)$$

where Ω is the element area and Γ is the element boundary.

3.2 Discretization of the pressure equation

To derive discretized pressure equation, the method of weighted residuals is applied to the continuity equation, Eq. (1),

$$\int_{\Omega} N_i \left(\frac{\partial U}{\partial X} + \frac{\partial V}{\partial Y} \right) d\Omega = - \int_{\Omega} \left(\frac{\partial N_i}{\partial X} U + \frac{\partial N_i}{\partial Y} V \right) d\Omega + \int_{\Gamma} N_i (U n_x + V n_y) d\Gamma = 0 \quad (10)$$

where, the integrations are performed over the element domain Ω and along the element boundary Γ ; n_x and n_y are the direction cosines of the unit normal to the element boundary with respect to X and Y directions respectively.

Now considering the following equations,

$$A_{ii} U_i = - \sum_{j \neq i} A_{ij} U_j + f_i^U - \int_{\Omega} N_i \frac{\partial P}{\partial X} d\Omega \quad (11a)$$

$$A_{ii} V_i = - \sum_{j \neq i} A_{ij} V_j + f_i^V - \int_{\Omega} N_i \frac{\partial P}{\partial Y} d\Omega \quad (11b)$$

where f_i^U and f_i^V are the surface integral terms and the source term due to buoyancy. By assuming constant pressure gradient on an element, it is evident that,

$$U_i = \bar{U}_i - K_i^P \frac{\partial P}{\partial X} \quad (12a)$$

$$V_i = \bar{V}_i - K_i^P \frac{\partial P}{\partial Y} \quad (12b)$$

where,

$$\bar{U}_i = \frac{1}{A_{ii}} \left(- \sum_{j \neq i} A_{ij} U_j + f_i^U \right) \quad (13a)$$

$$\bar{V}_i = \frac{1}{A_{ii}} \left(- \sum_{j \neq i} A_{ij} V_j + f_i^V \right) \quad (13b)$$

$$K_i^P = \frac{1}{A_{ii}} \left(\int_{\Omega} N_i d\Omega \right) \quad (13c)$$

By applying the element velocity interpolation functions from the Eqs. (7a) and (7b), into the continuity equation, Eq. (10), it follows that

10)

$$\int_{\Omega} \frac{\partial N_i}{\partial X} (N_j U_j) d\Omega - \int_{\Omega} \frac{\partial N_i}{\partial Y} (N_j V_j) d\Omega + \int_{\Gamma} N_i (U n_x + V n_y) d\Gamma = 0 \quad (14)$$

and introducing the nodal velocities U_j and V_j from Eqs. (12a) and (12b), ultimately Eq. (14) becomes,

$$\int_{\Omega} \frac{\partial N_i}{\partial X} (N_j K_j^F) \frac{\partial P}{\partial X} d\Omega + \int_{\Omega} \frac{\partial N_i}{\partial Y} (N_j K_j^F) \frac{\partial P}{\partial Y} d\Omega = \int_{\Omega} \frac{\partial N_i}{\partial X} (N_j \bar{U}_j) d\Omega + \int_{\Omega} \frac{\partial N_i}{\partial Y} (N_j \bar{V}_j) d\Omega - \int_{\Gamma} N_i (U n_x + V n_y) d\Gamma \quad (15)$$

Finally, by applying the element pressure interpolation functions, Eq. (7c), the above element equations can be written in matrix form with unknowns of the nodal pressures as,

$$(K_X + K_Y)P = F_U + F_V + F_C \quad (16)$$

where,

$$K_X = \int_{\Omega} \frac{\partial N_i}{\partial X} (N_j K_j^P) \frac{\partial N_k}{\partial X} d\Omega \quad (17a)$$

$$K_Y = \int_{\Omega} \frac{\partial N_i}{\partial Y} (N_j K_j^P) \frac{\partial N_k}{\partial Y} d\Omega \quad (17b)$$

$$F_U = \int_{\Omega} N_j \bar{U}_j \frac{\partial N_k}{\partial X} d\Omega \quad (17c)$$

$$F_V = \int_{\Omega} N_j \bar{V}_j \frac{\partial N_k}{\partial Y} d\Omega \quad (17d)$$

$$F_C = - \int_{\Gamma} N_i (U n_x + V n_y) d\Gamma \quad (17e)$$

The above element pressure equations are assembled to form the global equations; boundary conditions for the specified nodal pressures are imposed prior to solve for the updated nodal pressures

3.3 Discretization of the energy equation

The finite element equations corresponding to the energy equation are derived using an approach similar to that used in deriving elemental momentum equations. The standard Galerkin method is applied to yield the elemental equations which can be written in matrix form as,

$$K\theta + R \quad (18)$$

where, the matrix K consists of the known contributions from the convection and diffusion terms, and the load vectors R represent the heat flux along the element boundary as follows.

$$R = \frac{1}{\text{Re Pr}} \int_{\Gamma} N_i \left(\frac{\partial \theta}{\partial X} n_x + \frac{\partial \theta}{\partial Y} n_y \right) d\Gamma \quad (19)$$

These element equations are again assembled to yield the global temperature equations. Appropriate boundary conditions are applied prior to solve the new temperature values.

4. Results and Discussion

The numerical procedure used to solve the governing equations for the present work is the finite element method. The application of this technique is well documented by Zienkiewicz and Taylor [22]. Six noded triangular elements are used in this paper since the six noded elements smoothly capture the nonlinear variations of the flow and thermal field variables. Solutions were assumed to converge when the following convergence criteria was satisfied for every dependent variables at every point in the solution domain as,

$$\left| \frac{\Psi_{new} - \Psi_{old}}{\Psi_{old}} \right| \leq 10^{-6} \quad (20)$$

where, Ψ represents a dependent variable U , V , P , and θ .

Numerical experiments are performed in order to check the grid dependency of the solutions. There are four different grid (mesh) elements are used to test the grids as shown in Table 1. It is found that the solutions for different grid size are almost the same. Therefore, any grid size could be adopted. However, a relatively finer mesh (7162) has been adopted for the whole set of simulations.

There is no experimental results are reported in the literature as far as the authors concerned for this configuration. In order to validate the numerical code, the results were compared with those reported by Guo and Sharif [23]. In Figure 2, a comparison of the isotherms plot for Richardson number, $Ri = 10$ and discrete heat source size = 0.2 is presented. The agreement is found to be in acceptable range, which validates the present computations indirectly. Another validation is performed by comparing results with the experimental investigation of Corvaro and Paroncini [24] as cited in Table 2. The comparison shows reasonable well within experimental uncertainty.

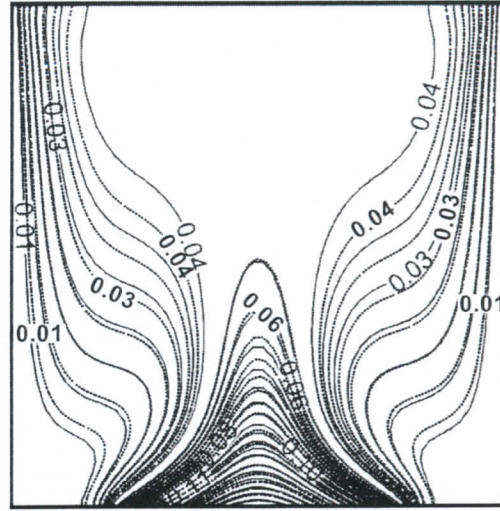


Figure 2: Comparison of the isotherms plot for Richardson number = 10 and discrete heat source size = 0.6 (solid line: Guo and Sharif [23] and dotted line: present)

Table 1: Comparison of Nu for various elements ($Ri = 10$, $\Phi = 0^\circ$)

Elements	4560	5924	7162	11906
Nu	6.1715	6.1721	6.1722	6.1722

Figure 3 shows the isotherms and streamlines plot for different Richardson numbers, when $\Phi = 0^\circ$ as a representative case. For all Richardson numbers, two large flat rotating cells are observed. The solution is symmetric about the vertical midline due to the symmetry of the problem geometry and boundary conditions. For $Ri = 0.1$, the flow descends downwards along the cold vertical sidewalls and turns horizontally to the central region after hitting the bottom wall. The flow then rises along the vertical symmetry axis and gets blocked at the centrally positioned adiabatic cylinder, which deflects the flow away from the vertical center line towards the cold vertical sidewalls. Thus the circulation of the flow shows two

Table 2: Comparison of Nu with experimental results

$(\text{RiRe}^2\text{Pr}) \times 10^{-4}$	7.56	13.8	17.1	19.8	23.2	25.0
Corvaro and Paroncini [24]	4.80	5.86	6.30	6.45	6.65	6.81
Present	5.31	6.07	6.37	6.58	6.82	6.94
Error (%)	10.63	3.60	1.11	2.01	2.56	1.91

overall rotating symmetric cells with two inner vortices respectively as shown in Figure 3 for the streamlines.

For $\text{Ri} = 1.0$, the patterns of the isotherms and streamlines are about the same as those for $\text{Ri} = 0.1$. However, a careful observation indicates that two upwelling cells appear on the upper corner of the adiabatic cylinder from the vertical centerline. A third cell appears above the top of the adiabatic cylinder with reverse direction owing to the two secondary vortices newly generated over the upper part of the adiabatic cylinder. As Ri increases further, the secondary two vortices over the top of the adiabatic cylinder decreases in size and finally disappears at $\text{Ri} = 10$ and accordingly, no third cell is found at this Ri .

Figure 4 shows the distribution of streamlines and isotherms for different Ri when $\Phi = 20^\circ$. When the inclination angle increases to 20° , the relative velocity of the circulating cells in the enclosure changes sharply and the isotherms are distorted more non-uniformly due to the weaker buoyancy effects, leading to the stratification of the isotherms. For dominating forced convection case with $\text{Ri} = 0.1$ (Figure 4), few small recirculating bubbles are also observed, one near the upper left corner above the primary bubbles. The cavity inclination has show a remarkable impact on the flow patterns along the vertical centerline except on the

isotherms until $\text{Ri} > 1$. For the mixed convection case with $\text{Ri} = 1$, the effect of cavity inclination is visible at the top corner of both sides where the recirculating bubbles at the upper left corner becomes weaker in size and stagnation of flow extent from left to right about the vertical centerline. With the increase of Ri , the cavity inclination has significant impact on the thermal and hydrodynamic flow fields. It is to be mentioned that the pure natural convection in a bottom heated horizontal cavity configuration is a thermally stratified stable formation and the flow physics is fundamentally different than that of an inclined cavity configuration. Thus, even though the shear driven flow is superimposed by the side lids, the thermal stratification in the bottom half of the cavity under the adiabatic cylinder is clearly visible in the isotherms for the horizontal cavity (Figure 3). The flow patterns and thermal field changes significantly with inclination for inclined cavities. The size of the primary recirculating bubble on the left is grown up and on the right is diminished as the inclination angle increases.

The overall Nusselt number at the heated surface, which is a measure of the overall heat transfer rate, is plotted in Figure 5 as a function of Richardson number. The effect of cavity inclination on the overall heat transfer process is clearly visible in this figure. It should be noted that in case of $\text{Ri} < 1$ is the forced

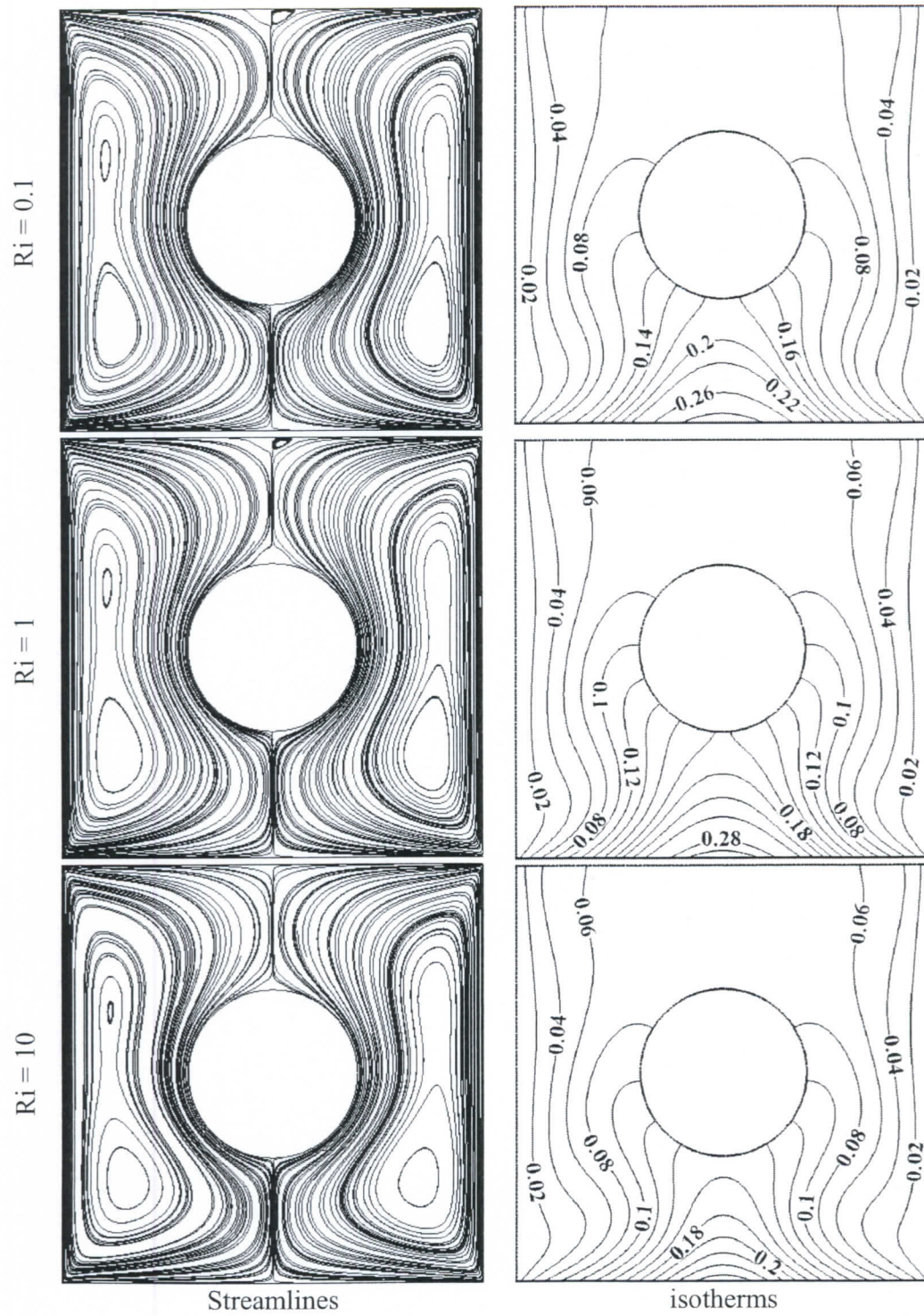


Figure 3: Variation of streamlines and isotherms for $\Phi = 0^\circ$.

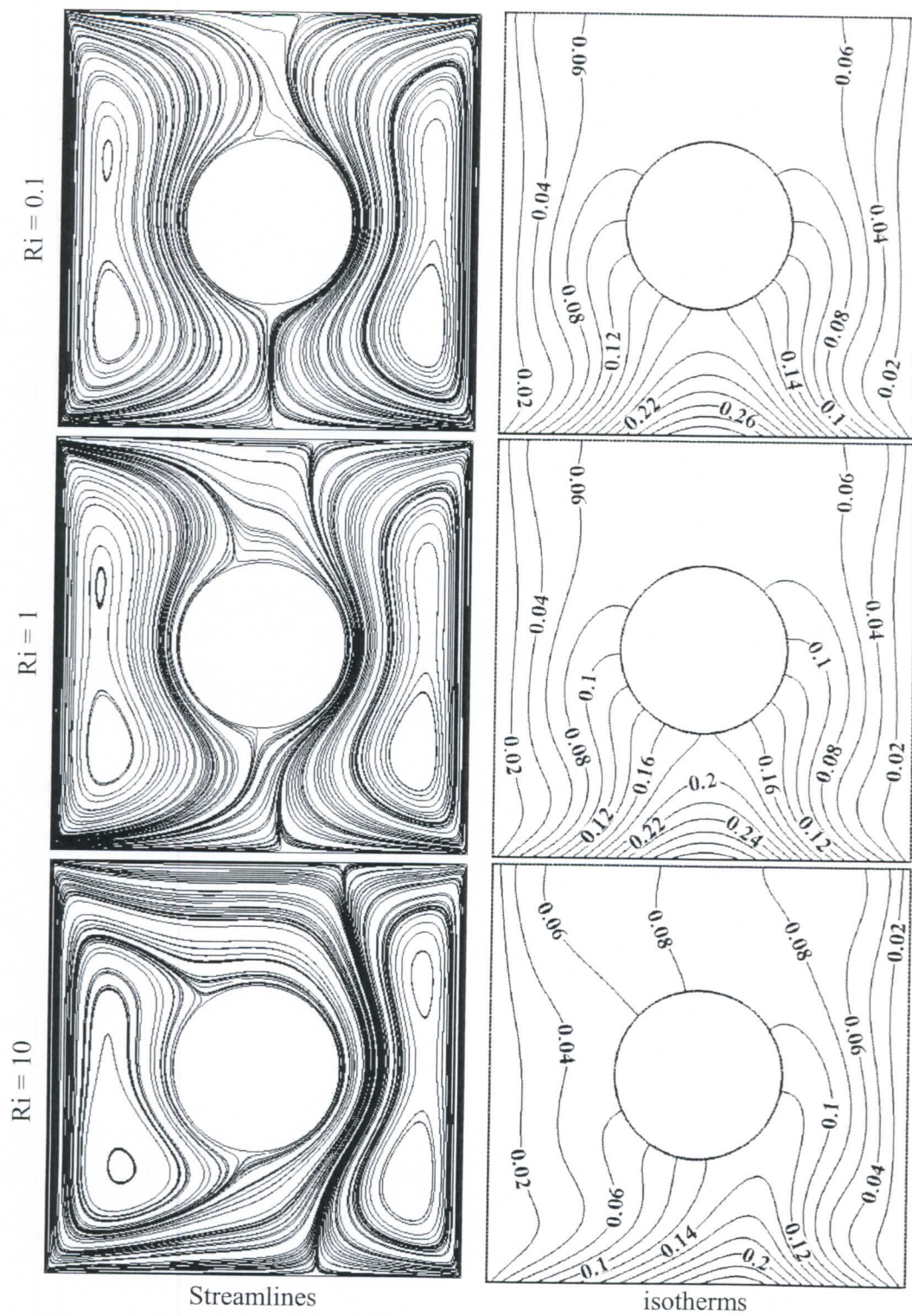


Figure 4: Variation of streamlines and isotherms for $\Phi = 20^\circ$.

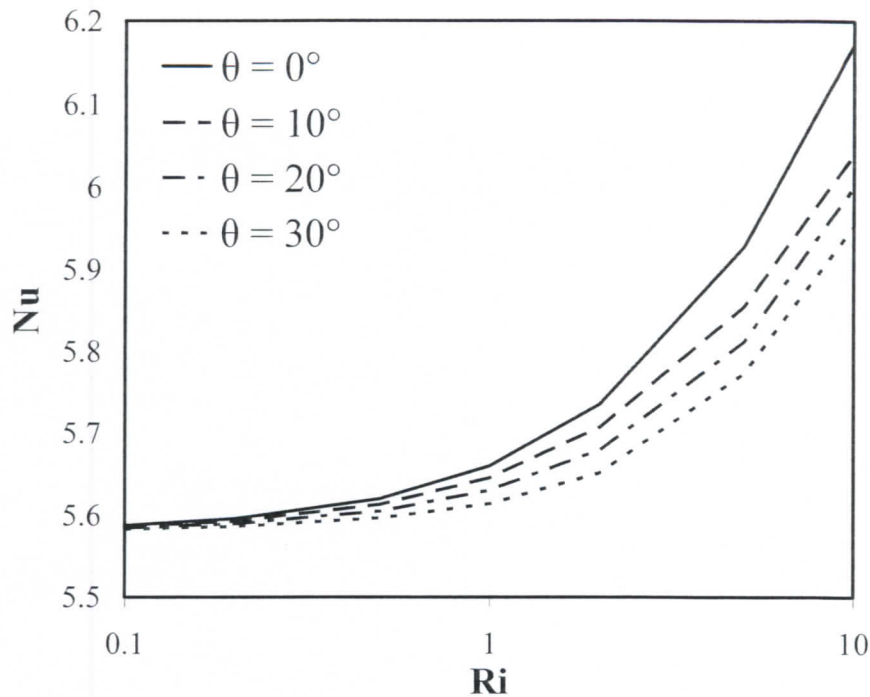


Figure 5: Variation of Nusselt number with the Richardson number.

convection dominated regime, for $Ri > 1$ is the natural convection dominated regime and $Ri = 1$ is the mixed one. It is seen here that for all cases the average Nusselt number variation as a function of Richardson number is very small within $Ri < 1$. The Nusselt number decreases gently with the increase of the cavity inclination angle for the dominating forced convection case, illustrating relative insensitivity of the overall heat transfer process with inclination angle. The horizontal cavity has a greater value of Nu compare to different inclined cavities due to very large buoyancy force.

5. Conclusions

The present work deals with the effect of the centrally positioned adiabatic cylinder on the heat transfer by mixed convection in a tilted lid-driven square enclosure heated uniformly at the bottom

by constant heat flux. The study is performed numerically by using combined finite element method. The results obtained for different inclination angles and for different Richardson numbers show that the flow and the heat transfer are affected by the adiabatic cylinder. A detailed analysis for the distribution of streamlines, isotherms and Nusselt number are carried out to investigate these effects. For all Richardson numbers considered in the present study, the flow and thermal fields eventually reach the steady state with the symmetric shape about the vertical centerline through the center of the inner circular cylinder. It has been observed that when Richardson number increases, the cavity inclination angle has significant impact on the thermal and hydrodynamic flow fields. Moreover, the results indicate that the horizontal cavity has a greater value of Nu compare to

different inclined cavities due to very large buoyancy force.

Nomenclature

A	Aspect ratio of the enclosure
c_p	Specific heat at constant pressure (kJ/kg .K)
g	Gravitational acceleration (m/s^2)
H	Height or width of the enclosure (m)
k	Thermal conductivity of fluid (W/m.K)
Nu	Nusselt number
p	Local pressure (N/m^2)
P	Dimensionless local pressure
Pr	Prandtl number
q	Heat flux at the heat source surface (W/m^2)
Ri	Richardson number
Re	Reynolds number
T	Temperature (K)
T_c	Temperature of the cold surface (K)
u	Dimensional velocity component in x-direction (m/s)
U	Dimensionless velocity component in x-direction
V_0	Constant speed (m/s)
v	Dimensional velocity component in y-direction (m/s)
V	Dimensionless velocity component in y-direction
x, y	Cartesian coordinates (m)
X, Y	Dimensionless Cartesian coordinates

Greek Symbols

α	Thermal diffusivity (m^2/s)
θ	Dimensionless temperature
ρ	Fluid density (kg/m^3)
β	Coefficient of volumetric expansion (K^{-1})
ν	Kinematic viscosity (m^2/s)
Φ	Inclination angle (degree)
Ψ	Dependent variable

References

- [1] Mohammad AA, Viskanta R
Transient low Prandtl number fluid convection in a lid-driven cavity. *Numer. Heat Transfer A*. Vol.19 (2): PP.187-205, 1991.
- [2] Moallemi MK, Jang KS
Prandtl number effects on laminar mixed convection heat transfer in a lid-driven cavity. *Int. J. Heat Mass transfer*. Vol. 35: PP. 1881-1892, 1992.
- [3] Iwatsu R, Hyun JM, Kuwahara K
Mixed convection in a driven cavity with a stable vertical temperature gradient. *Int. J. Heat Mass Transfer*. Vol. 36: PP. 1601-1608, 1993.
- [4] Iwatsu R and Hyun JM, Three-dimensional driven cavity flows with a vertical temperature gradient. *Int. J. Heat Mass transfer*. Vol. 38: PP. 3319-3328, 1995.
- [5] Mansour RB, Viskanta R, Shear-opposed mixed convection flow heat transfer in a narrow vertical cavity. *Int. J. Heat Fluid Flow*. Vol.15: PP. 462-469, 1994.
- [6] Prasad AK, Koseff JR, Combined forced and natural convection heat transfer in a deep lid-driven cavity flow. *Int. J. Heat Fluid Flow*. Vol. 17: PP. 460-467, 1996.
- [7] Kuhlmann HC, Wanschura M, Rath HJ, Flow in two sided lid-driven cavities: non-uniqueness, instabilities, and cellular structures. *J. Fluid Mech*. Vol. 336: PP. 267-299, 1997.
- [8] Alleborn N, Raszillier H, Durst F, Lid-driven cavity with heat and mass transport. *Int. J. Heat Mass Transfer*. Vol.42: PP. 833-853, 1999.
- [9] Khanafer K, Chamkha AJ, Mixed convection flow in a lid-driven enclosure filled with a fluid saturated porous medium, *Int. J. Heat Mass Transfer*. Vol.42: PP. 2465-2481, 1999.
- [10] Shankar PN, Meleshko VV, Nikiforovich EI, Slow mixed convection in rectangular containers. *J. Fluid Mech*. Vol. 471: PP. 203-217, 2002.
- [11] Oztop HF and Dagtekin I, Mixed convection in a two-sided lid-driven differentially heated square cavity. *Int. J. Heat Mass Transfer*. Vol.47: PP. 1761-1769, 2004.
- [12] Larson DW, Gartling DK, Schimmel WP, Natural convection studies in nuclear spent-fuel shipping casks. *Computation and Experiment, J. Energy*. Vol. 2(3), 1993.
- [13] Roychowdhury DG, Das SK, Sundararajan TS, Numerical simulation of natural convective heat transfer and fluid flow around a heated cylinder inside an enclosure. *Heat Mass Transfer*. Vol. 38: PP. 565-576, 2002.
- [14] Elepano AR and Oosthuizen PH, Free convective heat transfer from a heated cylinder in an enclosure with a cooled upper surface, in: Wrobel LC, Brabbia CA, Nowak AJ (Eds.). *Advanced Computational Methods in Heat Transfer 2*. Computational Mechanics Publication, Southampton, Boston, 1990.

- [15] Kim BS, Lee DS, Ha MY, Yoon HS, A numerical study of natural convection in a square enclosure with a circular cylinder at different vertical locations. *Int. J. Heat Mass Transfer*. Vol. 51: PP.1888–1906, 2008.
- [16] Misirlioglu A, The effect of rotating cylinder on the heat transfer in a square cavity filled with porous medium. *Int. J. Eng. Scie* 44: PP. 1173–1187, 2006.
- [17] Hussain SH and Hussein AK, Numerical investigation of natural convection phenomena in a uniformly heated circular cylinder immersed in square enclosure filled with air at different vertical locations. *Int Commun. Heat Mass Transfer*. Vol.37: PP.1115–1126, 2010.
- [18] Kuehn TH and Goldstein RJ, An experimental study and theoretical study of natural convection in the annulus between horizontal concentric cylinders. *J. Fluid Mech*. Vol.74: PP. 695–719, 1976.
- [19] Projahn U, Rieger H, Beer H, Numerical analysis of laminar natural convection between concentric and eccentric cylinders. *Numer. Heat Transfer*. Vol.4: PP. 131–146, 1981.
- [20] Sasaguchi K, Kuwabara K, Kusano K, Kitagawa H, Transient cooling of water around a cylinder in a rectangular cavity – a numerical analysis of the effect of the position of the cylinder. *Int. J. Heat Mass Transfer*. Vol.41: PP. 3149–3156, 1998.
- [21] Saha S, Saha G, Islam MQ, Natural convection in square enclosure with adiabatic cylinder at center and discrete bottom heating. *Daffodil Int. University J. Sci. Tech*. Vol. 3(1): PP. 29–36, 2008.
- [22] Zienkiewicz OC and Taylor RL, *The finite element method*, 5th edn. Oxford: Butterworth-Heinemann, 2000.
- [23] Guo G and Sharif AR, Mixed convection in rectangular cavities at various aspect ratios with moving isothermal sidewalls and constant flux heat source on the bottom wall. *Int. J. of Thermal Sciences*. Vol.43:PP.465-475, 2004.
- [24] Corvaro, F and Paroncini, M, A numerical and experimental analysis on the natural convection heat transfer of a small heating strip located on the floor of a square cavity. *Applied Thermal Engineering*. Vol. 28: PP. 25-35, 2008.